Journal of Organometallic Chemistry 694 (2009) 2858–2865

Contents lists available at ScienceDirect

Journal of Organometallic Chemistry

journal homepage: www.elsevier.com/locate/jorganchem

$[Ni(P_2^{Ph}N_2^{Ar})_2(NCMe)][BF_4]_2$ as an electrocatalyst for H_2 production: $P_2^{Ph}N_2^{Ar}$ = 1,5-(di(4-(thiophene-3-yl)phenyl)-3,7-diphenyl-1,5-diaza-3,7-diphosphacyclooctane)

Douglas H. Pool [1], Daniel L. DuBois *

Pacific Northwest National Laboratory, P.O. Box 999, Richland, WA 99352, United States
Pacific Northwest National Laboratory, 908 Battelle Blvd., MS K2-57, Richland, WA 99354, United States

ARTICLE INFO

Article history:
Received 27 February 2009
Received in revised form 3 April 2009
Accepted 7 April 2009
Available online 17 April 2009

Keywords:
Hydrogen production
Nickel
Catalyst

ABSTRACT

A new cyclic 1,5-diaza-3,7-diphosphacyclooctane ligand was prepared with phenyl substituents on phosphorus and (thiophene-3-yl)phenyl substituents on nitrogen. This ligand reacts with $[Ni(CH_3CN)_6][BF_4]_2$ to form the corresponding $[Ni(P_2^{Ph}N_2^{Ar})_2(NCMe)][BF_4]_2$ complex, **3**, which is an active electrocatalyst for H_2 production. Kinetic studies indicate that the catalytic rate is first order in catalyst and second order in acid at low concentrations of acid, but at higher acid concentrations the catalytic rate becomes independent of acid concentration. The rate-determining step at high acid concentrations is attributed to the elimination of H_2 from a reduced Ni species. The modest overpotential of 280 mV and a turnover frequency of 56 s^{-1} confirm that **3** is a relatively active catalyst for H_2 production in acetonitrile solutions. Oxidation of the pendant thiophene substituents of **3** results in the formation of films on glassy carbon electrode surfaces. However these films are not electroactive, and electrocatalysis of proton reduction is not observed with these modified electrodes.

1. Introduction

With the increasing use of alternative energy sources such as nuclear, wind, and solar will come the need for an effective means to store and transport the electrical energy produced by these sources. One such energy carrier is hydrogen gas that can be generated in a variety of ways including electrolysis [1]. Platinum metal is an excellent catalyst for the generation of hydrogen as well as the oxidation of hydrogen in fuel cells, but its cost and limited distribution provide strong incentives for the development of catalysts based on more abundant and less expensive metals. The hydrogenase enzymes found in nature catalyze hydrogen production and oxidation using the far more abundant elements of nickel and iron in the active site [2–7]. A drawing of a proposed structure of the [FeFe] hydrogenase active site based on X-ray diffraction studies [5] is shown by structure **1**.

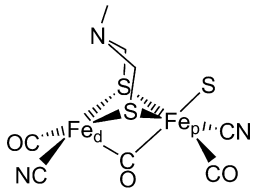

1

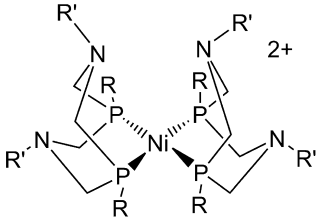

2a R = Cy R' = Benzyl (Bz)
2b R = Ph R' = Bz
2c R = Ph R' = Ph

A series of nickel complexes using cyclic 1,5-diaza-3,7-diphosphacyclooctane ligands of the general formula $[Ni(P_2^RN_2^{R'})_2]^{2+}$,

* Corresponding author. Tel.: +1 509 375 2331.
E-mail addresses: douglas.pool@pnl.gov (D.H. Pool), daniel.dubois@pnl.gov (D.L. DuBois).
[1] Tel.: +1 509 372 4938.

0022-328X/$ - see front matter © 2009 Elsevier B.V. All rights reserved.
doi:10.1016/j.jorganchem.2009.04.010

structure **2**, catalyze the electrochemical production or oxidation of hydrogen [8–13]. The cyclic diphosphine ligands coordinate to the metal through the two phosphorus atoms leaving the nitrogens as pendant bases similar to that proposed for the [FeFe] hydrogenase. The substituents on the $P_2^RN_2^{R'}$ ligand tune the ability of these complexes to bind or release H_2 in a heterolytic manner. Variations at the phosphine position affect the hydride acceptor ability of the Ni center, while the groups at the nitrogen position affect the pK_a of the protonated base formed during the catalytic cycle [11,12–18]. The complex $[Ni(P_2^{Cy}N_2^{Bz})_2]^{2+}$ (**2a**) is a hydrogen oxidation catalyst [9], $[Ni(P_2^{Ph}N_2^{Bz})_2]^{2+}$ (**2b**) is a better hydrogen production than oxidation catalyst [11], and $[Ni(P_2^{Ph}N_2^{Ph})_2]^{2+}$ (**2c**) is the best hydrogen production catalyst of the series [10]. Particularly interesting features of these catalysts are their relatively high catalytic rates with modest overpotentials and their lack of inhibition by CO [9,19].

For practical reasons it is ultimately desirable for these molecular catalysts to be attached to electrode surfaces [20]. There are a number of methods that have been studied for electrode modification [20–25], and in this paper we explore one of these, the electrochemical generation of a polythiophene. Thiophene is susceptible to oxidation, generating radicals that combine to form polymers that precipitate at the electrode surface. Lennox and coworkers demonstrated the ability to polymerize thiophenes with tethered ferrocene groups that were redox active once confined to the electrode surface [24]. In this work, we describe the synthesis of a new 1,5-diaza-3,7-diphosphacyclooctane ligand with thiophene groups attached to the pendant nitrogen base and a corresponding nickel complex. The resulting complex was investigated for its ability to form coatings on electrode surfaces with redox active Ni. Additionally the complex was used in solution to investigate its ability to reduce protons. The resulting data allows for a comparison to similar complexes and contributes to a broader understanding of the $[Ni(P_2^RN_2^{R'})_2]^{2+}$ series.

2. Results

2.1. Synthesis

The thiophene substituted aniline, 4-(thiophen-3-yl)aniline, reacts with $PhP(CH_2OH)_2$ in acetonitrile to give an off-white solid with limited solubility. Because of the low solubility, it was characterized by solid state ^{31}P NMR spectroscopy and found to have a single resonance at −37.3 ppm. The material is partially soluble in DMSO-d_6 and the ^{31}P NMR spectrum of the resulting solution has a main resonance at −49.3 ppm and a small resonance at −35.2 ppm, tentatively assigned to isomers with *cis* and *trans* phenyl groups with respect to the cyclooctane ring. This white powder reacts with $[Ni(NCMe)_6][BF_4]_2$ in acetonitrile to give a red solution of $[Ni(P_2^{Ph}N_2^{Ar})_2(NCMe)][BF_4]_2$ (**3**) (where $P_2^{Ph}N_2^{Ar}$ is 1,5-(di(4-(thiophene-3-yl)phenyl)-3,7-diphenyl-1,5-diaza-3,7-diphosphacyclooctane) after four days of stirring (Scheme 1), consistent with the proposed structure of the ligand [26]. Crystals of **3** form readily with the diffusion of ethyl ether into acetonitrile, and the purity was confirmed by elemental analysis. The proton NMR spectrum contains a series of distinct resonances in the aromatic region and two doublets at 4.29 and 3.98 ppm consistent with two sets of aliphatic methylene groups expected for a bicyclic ligand. Decoupling experiments and integration allow for the chemical shift assignments listed in Section 5 and consistent with structure **3**. The ^{31}P NMR spectrum of **3** recorded in acetonitrile-d_3 consists of a single resonance at 5.0 ppm similar to the value of 4.8 ppm reported for **2c**, which has been characterized by an X-ray diffraction study [9].

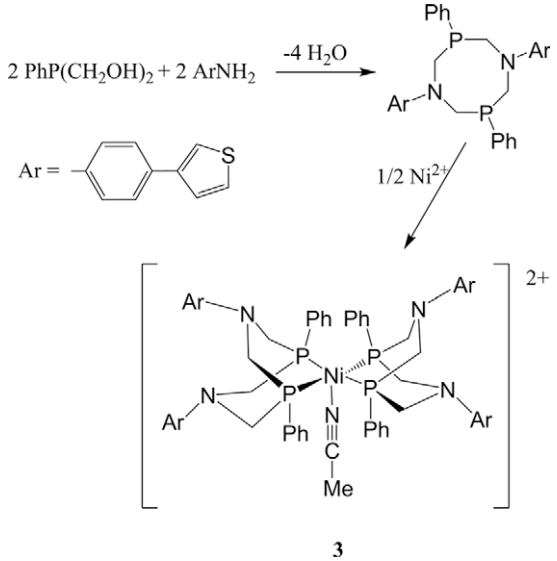

3

Scheme 1.

2.2. Electrochemical studies

The cyclic voltammogram of **3** in benzonitrile has two reversible one-electron waves with $E_{1/2}$ = −0.80 V (with a peak to peak separation (ΔE_p) of 56 mV) and $E_{1/2}$ = −0.99 V (ΔE_p = 62 mV). Plots of the peak currents of these waves vs. the square root of the scan rate are linear indicating the electron transfers are diffusion controlled. These two waves correspond to Ni(II/I) and Ni(I/0) couples. When the cyclic voltammogram of **3** is recorded in acetonitrile, the Ni(II/I) wave is at $E_{1/2}$ = −0.82 V (ΔE_p = 59 mV). At low concentrations of **3**, the Ni(I/0) wave is observable at $E_{1/2}$ = −1.01 V (ΔE_p = 58 mV) (Fig. 1). The Ni(I/0) couple becomes a stripping wave at concentrations greater than 0.7 mM in **3** in acetonitrile as a result of precipitation of the Ni(0) complex on the electrode surface. The cyclic voltammogram of **3** also exhibits irreversible oxidation waves at potentials more positive than +0.6 V.

Complex **3** appears to polymerize onto the working electrode at potentials greater than 0.6 V during cyclic voltammetry experiments. Multiple sweep cyclic voltammograms in which the potential excursions remain negative of 0.6 V exhibit little or no decrease in peak currents for the solution based Ni(II/I) and Ni(I/0) waves as well as the oxidation current observed between 0.4 and 0.6 V. Cycling to potentials greater than 0.6 V results in a decrease in

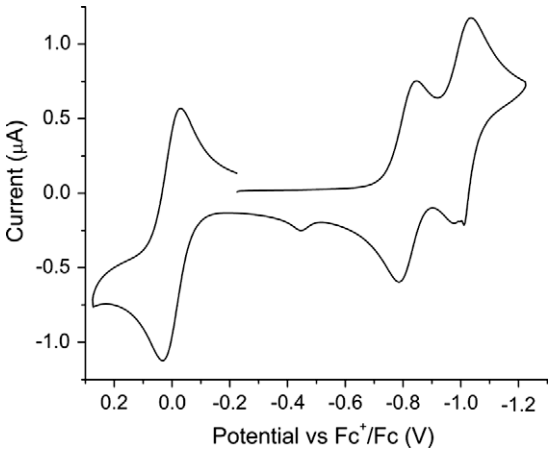

Fig. 1. Cyclic voltammogram of a 0.7 mM solution of **3** in acetonitrile containing 0.2 M NEt_4BF_4 using a scan rate of 50 mV/s with a 1 mm diameter glassy carbon working electrode. The wave at 0.00 V corresponds to the ferrocenium/ferrocene couple arising from added ferrocene, which was used as the internal standard.

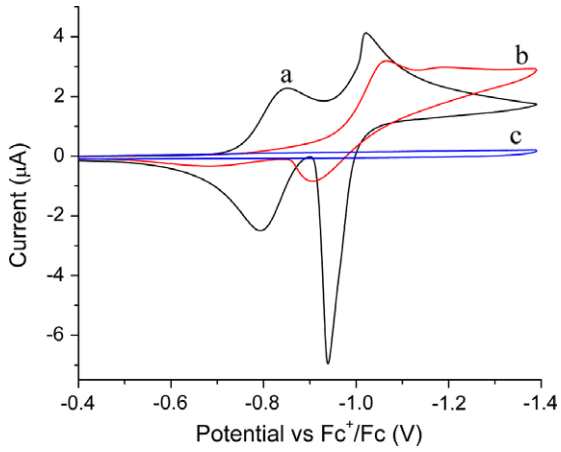

Fig. 2. Cyclic voltammograms of a 1.1 mM **3** and 0.1 M NEt_4BF_4 acetonitrile solution using a glassy carbon working electrode scanned at 0.1 V/s showing the Ni(II/I) and Ni(I/0) reductions in solution: with a clean working electrode showing stripping waves (a); after the potential was cycled from −0.4 V to 0.8 V and back to −0.4 V at 0.1 V/s (b); after the potential was cycled from −0.4 V to 1.1 V and back to −0.4 V again at 0.1 V/s (c).

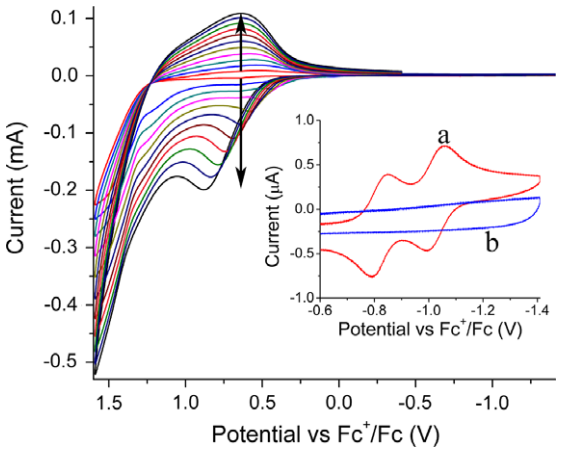

Fig. 4. Ten consecutive cyclic voltammograms scanning from −0.4 V to −1.4 V, then positive to 1.6 V, and back to −0.4 V of an acetonitrile solution containing 0.6 mM **3**, 20 mM thiophene, and 0.1 M NEt_4BF_4. The working electrode was glassy carbon, and the scan rate was 0.1 V/s. The first scan shows the Ni(II/I) and Ni(I/0) couples of **3** in solution (a, inset) while the second scan no longer does (b, inset).

the current observed for the Ni(II/I) and Ni(I/0) waves of **3** in solution on subsequent sweeps to negative potentials (Fig. 2). The oxidation current observed in sequential scans to greater than 0.6 V also decreases. Additionally when ferrocene is included in the solution as an internal reference, the return reduction wave for the Fe(III/II) couple decreases after an initial sweep to positive potentials, and the reduction wave is much broader with lower peak currents indicating the process is no longer diffusion controlled (Fig. 3, trace a). This decrease in reduction current for the ferrocene couple is not observed for cyclic voltammograms of the closely related complex, $[Ni(P_2^{Ph}N_2^{Ph})_2NCMe][BF_4]_2$ (**2c**), that lacks the thiophene group, and which also has non-reversible oxidation peaks at potentials more positive than 0.7 V (Fig. 3, trace b). When the working electrode is coated by cycling to potentials greater than 0.7 V in a solution of **3**, removed from solution, placed in a separate electrochemical cell with only electrolyte, and cycled between 0.0 and −1.4 V, no current is observed for the Ni(II/I) and Ni(I/0) couples. The addition of cobaltocenium hexafluorophosphate to the solution resulted in the observation of the Co(III/II) couple but no mediated charge transfer for the reduction of nickel complexes confined to the surface, as would be indicated by a ratio of cathodic to anodic currents of greater than 1.0 [27–29]. While conducting the same experiments with a mixture of 20:1 thiophene:**3** shows increased current between −0.4 and 1.6 V with consecutive scans associated with the formation of polythiophene (Fig. 4), they failed to show any electrochemically active nickel species confined to the electrode surface (Fig. 4 inset).

2.3. Electrocatalytic production of hydrogen

Although complex **3** does not remain electrochemically active when attached to the electrode surface, **3** in acetonitrile solutions does catalyze the reduction of protons from *p*-cyanoanilinium tetrafluoroborate at −0.83 V vs. the ferrocenium/ferrocene couple (Fig. 5). This is indicated by the large increase of the current at the potential of the Ni(II/I) couple of **3** in the presence of the acid *p*-cyanoanilinium tetrafluoroborate. Two important parameters for such a catalytic process are the overpotential and the catalytic rate. The pK_a of *p*-cyanoanilinium tetrafluoroborate in acetonitrile is 7.0 [30], and using a potential of −0.14 V for the NHE vs. the ferrocenium/ferrocene couple in acetonitrile [31], the approximate potential required for proton reduction with this acid is −0.55 V.

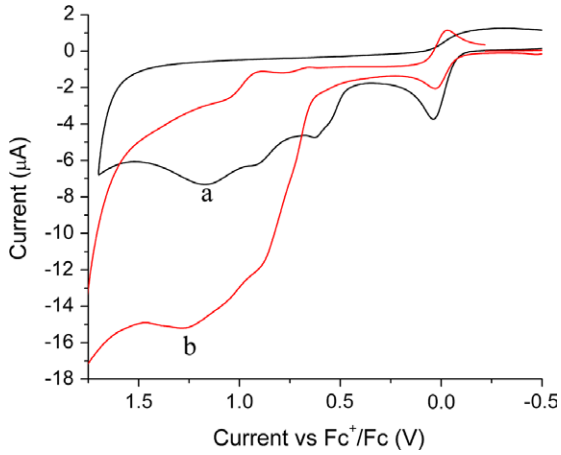

Fig. 3. CV experiments for 0.9 mM **3** (a) in benzonitrile with 0.2 M NBu_4BF_4 and 0.7 mM **2c** (b) in acetonitrile with 0.2 M NEt_4BF_4. Both experiments have added ferrocene as an internal reference and a scan rate of 0.1 V/s using a 1 mm diameter glassy carbon working electrode.

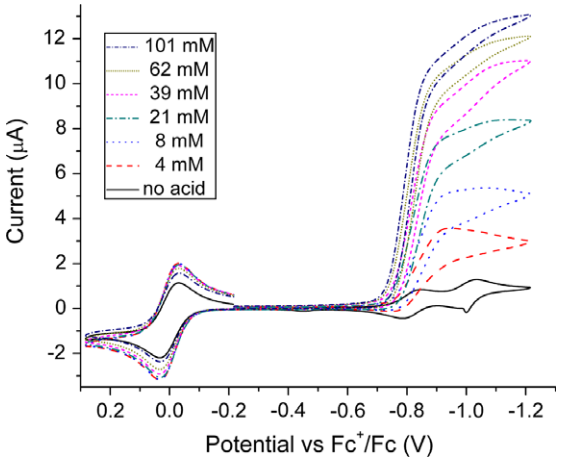

Fig. 5. Cyclic voltammograms recorded on an acetonitrile solution containing 0.73 mM **3** and 0.2 M NEt_4BF_4 with added ferrocene as a function of acid (*p*-cyanoanilinium tetrafluoroborate) concentration. The scan rate was 50 mV/s with a glassy carbon working electrode.

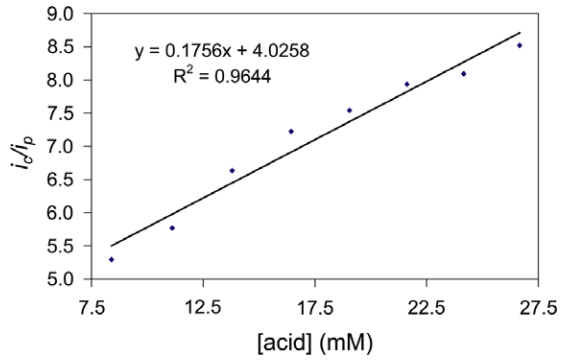

Fig. 6. Plot of the ratio of the catalytic current (i_c) to the peak current of the Ni(II/I) couple in the absence of acid (i_p) as a function of the concentration of *p*-cyanoanilinium tetrafluoroborate at low acid concentrations. The solution was 0.66 mM **3** and 0.2 M NEt_4BF_4 in acetonitrile, the scan rate was 50 mV/s, and the working electrode was glassy carbon.

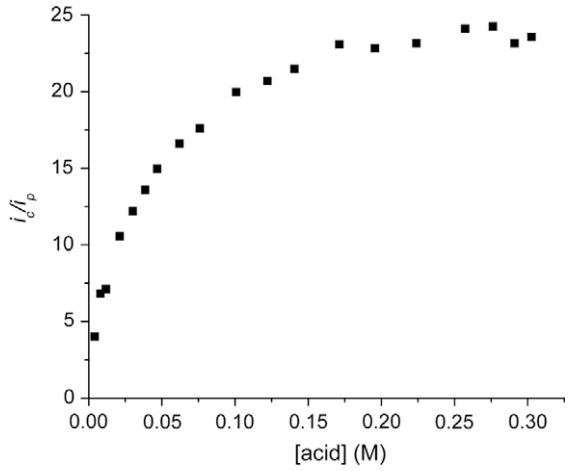

Fig. 7. Plot of the ratio of the catalytic current (i_c) to the peak current of the Ni(II/I) couple in the absence of acid (i_p) as a function of the concentration of *p*-cyanoanilinium tetrafluoroborate. The solution was 0.73 mM **3** and 0.2 M NEt_4BF_4 in acetonitrile, the scan rate was 50 mV/s, and the working electrode was glassy carbon.

This gives an estimated overpotential of 0.28 V for the catalytic reduction of the protons of *p*-cyanoanilinium tetrafluoroborate using **3** as the catalyst. Information on the catalytic rate can be obtained by plotting the ratio of the observed catalytic current (i_c) to the current of the Ni(II/I) reduction in the absence of acid (i_p) vs. the concentration of acid [9,11,32–34]. The straight line observed at lower acid concentrations (Fig. 6) indicates the reaction is second order in acid. A similar plot of i_c verses the concentration of **3** gives a straight line indicating a first order dependence on catalyst [32–34]. At acid concentration greater than approximately 0.2 M, the rate of reaction becomes independent of the acid concentration (Fig. 7).

A mechanism is shown in Scheme 2 that is consistent with the observations described above and with previous studies of similar complexes for both H_2 production and oxidation [9,10,32]. In this catalytic cycle, step 6 is the rate-determining step. Step 6 is the reductive elimination of H_2. There are two electron transfer steps (1 and 3) and two protonation steps (2 and 4) that precede this step. These two protonation steps will be governed by equilibria that determine the fraction of the complex that is in the doubly protonated Ni^0 form, $[Ni(P^R_2N^{R'}HN^{R'})_2]^{2+}$. As a result the rate of the catalytic reaction is expected to obey Michaelis–Menton kinetics with the rate expression shown in Eq. (1) where k_4 and k_{-4} may actually be a composite of forward and reverse rate constants for step 2 as well. The equation for catalytic current, i_c, for cyclic voltammetry is given by Eq. (2) where n is the number of electrons consumed in the catalytic cycle, F is the Faraday constant, $[Cat]_T$ is the total or initial concentration of the catalyst, D is the diffusion coefficient of the catalyst, and k_{obs} is the observed rate constant for the particular catalytic reaction under consideration [33–35]. The derivation of this equation assumes that the concentration of the substrate, BH^+, is sufficiently large that it remains constant at the initial value of the bulk solution. The value of n in Eq. (2) will be

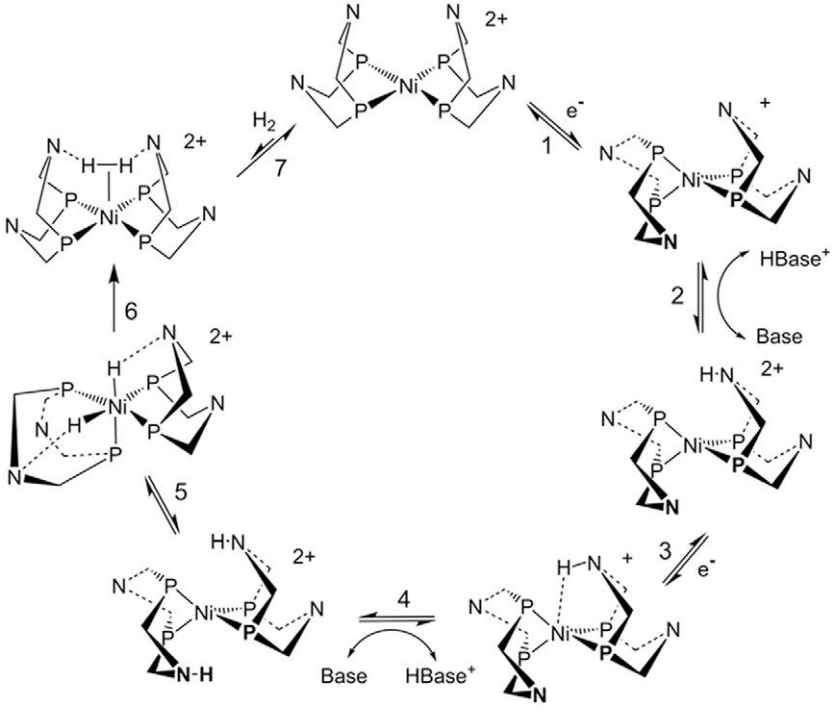

Scheme 2.

2.0 because two electrons are consumed in the catalytic cycle (steps 1 and 3). Similarly, the expression for the peak current for a reversible n'-electron reduction is given by Eq. (3). In this equation n' will be 1.0 because the wave at −0.8 V in the absence of acid corresponds to a simple reversible one-electron process. Substitution of k_{obs} from Eq. (1) into Eq. (2) and dividing the result by Eq. (3) gives Eq. (4). At low acid or protonated base (BH^+) concentrations, Eq. (4) indicates a linear dependence will be observed for i_c/i_p, as observed experimentally. At these low concentrations the observed rate constant is a composite of constants for several elementary steps. At high concentrations of BH^+, Eq. (4) simplifies to Eq. (5) and the observed rate constant corresponds to the simple unimolecular elimination of H_2 for step 6. Using Eq. (5) a rate constant of 56 s^{-1} can be obtained for step 6 from the data in the acid independent region of the plot shown in Fig. 7. This number represents the number of times a catalyst molecule produces a molecule of H_2 in a second, or the turnover frequency of this catalyst under these conditions. At intermediate concentrations of BH^+, the reaction order for this species will change from second to zero order in acid (BH^+) and the catalytic current will change from first to zero order as observed in Fig. 7.

$$\text{rate} = \frac{k_6[BH^+]^2}{\frac{k_{-4}+k_6}{k_4} + [BH^+]^2}[\text{Cat}]_T = k_{obs}[\text{Cat}]_T \quad (1)$$

$$i_c = nFA[\text{Cat}]_T(Dk_{obs})^{1/2} \quad (2)$$

$$i_p = 0.446n'FA[\text{Cat}]_T(Dv)^{1/2}(n'F/RT)^{1/2} \quad (3)$$

$$\frac{i_c}{i_p} = \frac{2}{0.446}\sqrt{\left(\frac{RT}{Fv}\right)\frac{k_6[BH^+]^2}{\frac{k_{-4}+k_6}{k_4} + [BH^+]^2}} \quad (4)$$

$$\frac{i_c}{i_p} = \frac{2}{0.4463}\sqrt{\frac{RTk_6}{Fv}} \quad (5)$$

3. Discussion

Complex **3** was prepared for two reasons. First, only three derivatives of complexes of type **2** have been prepared previously [9,11]. Although the complex $[Ni(P_2^{Ph}N_2^{Ph})_2]^{2+}$ (**2c**) is a good catalyst for H_2 production with high catalytic rates (350 s^{-1}) and moderate overpotentials (330 mV) [10,11], it is important to further determine how changes in ligand substituents affect catalytic properties. Second, the attachment of a thiophene substituent to the cyclic diphosphine ligand could provide a convenient route for electrode modification with these catalysts by electrochemically polymerizing the thiophene substituent of the catalyst with itself to form oligomers. Alternatively, a more extensive poly-thiophene chain might be formed by copolymerization of **3** and thiophene. The inhibition of ferrocenium reduction after complex **3** is oxidized at potentials positive of 0.6 V is consistent with the formation of an insulating layer on the working electrode. Because complex **2a** also exhibits irreversible oxidations at similar positive oxidation potentials, but does not impede charge transfer between the working electrode and ferrocenium ions in solution as observed for **3**, it is reasonable to assume the thiophene substituents are involved in the polymerization. While polymerization or oligomerization appears to confine the coordinated nickel species to the surface of the electrode, efforts to observe any redox activity of the confined species at potentials close to those of the Ni(II/I) or Ni(I/0) couples of the complex in solution failed, including the use of thiophene copolymerization and mediation with $CoCp_2BF_4$. One possible explanation for this behavior is that polymerization restricts the diffusion of the nickel catalyst to the electrode surface thereby preventing electron transfer. However, cobaltocenium reduction to cobaltocene is observed, and the cobaltocene produced in solution by electron transfer does not appear to mediate nickel reduction as would be indicated by an enhanced reduction current. Another possibility is that reduction of nickel is not observed because the nickel complex is not able to undergo structural rearrangements from square planar or trigonal bipyramidal Ni(II) complexes [9] to tetrahedral Ni(I) and Ni(0) species that typically occur upon reduction of Ni(II) complexes [36]. This may be the result of multiple thiophene substituents per Ni(II) complex being incorporated into the resulting polymer or simple physical restriction of this motion by the backbone of the polymer. Finally, because the oxidation of **3** is irreversible, the oxidation process itself may also destroy the catalyst as it is polymerized. Whatever the reason, the use of thiophene modified complexes does not result in electrochemically active species confined to the electrode surface.

Although the thiophene groups of **3** did not work well as a means to modify electrodes, it did demonstrate that adding substituents to the *para* position in the aniline portion of the ligand system does not dramatically change the electrochemistry of the nickel center in solution. When the cyclic voltammograms of **2c** and **3** in acetonitrile are compared, the values for the Ni(II/I) waves are found to be very similar, with a small positive shift of 20 mV for **3** compared to **2c**. The Ni(I/0) waves have an even smaller measured difference of +10 mV for **3** compared to **2c**. As indicated in Section 5, the pK_a for the 4-(thiophen-3-yl)aniline was determined by measuring the equilibrium constant for the reaction with anilinium tetrafluoroborate. This equilibrium constant was used to calculate a pK_a value of 10.3 for 4-(thiophen-3-yl)anilinium tetrafluoroborate based on a pK_a value of 10.62 for anilinium tetrafluoroborate [37]. This is fully consistent with the small positive shifts in the Ni(II/I) and Ni(I/0) potentials upon replacing hydrogen in **2c** with a thiophene substituent in **3**.

Hydrogen production catalyzed by **3** using the weak acid *p*-cyanoanilinium tetrafluoroborate was consistent with the behavior reported for $[Ni(P_2^{Ph}N_2^{Ph})_2NCMe]^{2+}$ (**2c**) [9,10]. The reaction is first order in catalyst and second order in acid concentration at lower concentrations. At high acid concentrations the rate of reaction becomes acid independent, and the rate of this reaction corresponds to the loss of H_2 from the reduced form of the catalyst. The rate of 56 s^{-1} observed for **3** is somewhat less than the rates of 350 s^{-1} observed for **2c** [10] and 700 s^{-1} reported for Ni–Fe hydrogenases [2]. The driving force for this reaction depends on the hydride donor ability of the nickel hydride $[HNi(P_2^RN_2^{R'})_2]^+$ and the pK_a of the protonated N–Ar group in the H_2 adduct $[Ni^0(P_2^RN^{R'}HN^{R'})_2]^{2+}$ [11]. Based on a comparison of the potentials of the Ni(II/I) couples of **2c** and **3**, the corresponding hydride of complex **3**, $[HNi(P_2^{Ph}N_2^{Ar})_2]^+$, should be a slightly weaker hydride donor than $[HNi(P_2^{Ph}N_2^{Ph})_2]^+$ (0.02 V × 19.2 kcal/V mol = 0.38 kcal/mol) [11]. Similarly, the slightly lower pK_a value of 4-(thiophen-3-yl)anilinium tetrafluoroborate compared to anilinium tetrafluoroborate would suggest a slightly more acidic NH proton for catalyst **3** compared to **2c** ($2.303RT[10.62–10.34]$) = 0.38 kcal/mol). As a result catalyst **3** would be expected to be slightly less hydridic (by 0.38 kcal/mol) and slightly more acidic than **2c** (by 0.38 kcal/mol). Because these two effects (hydride donor abilities and acidities) are in opposite directions, similar driving forces for H_2 loss are expected for **2c** and **3**. It should also be noted that **3** has a slightly lower overpotential of 280 mV compared to 330 mV required for **2c** that should favor a slightly higher rate for H_2 production by **2c**.

4. Summary

A new thiophene substituted catalyst of the type $[Ni(P_2^{Ph}N_2^{Ar})_2]^{2+}$ (where Ar = 4-(thiophen-3-yl)phenyl) has been prepared and

characterized. Although the thiophene substituted complex **3** has not resulted in electrochemically active modified electrodes in our hands, this complex is still a very active catalyst for H_2 production in acidic acetonitrile solutions with an overpotential of 280 mV and a turnover frequency of 56 s^{-1}. This combination of high activity and modest overpotentials confirms that the high activity observed is a general feature of this class of complexes. High activities for electrocatalytic H_2 production or oxidation can be expected for similar complexes with a variety of substituents on both phosphorus and nitrogen.

5. Experimental

5.1. General methods

Acetonitrile from Alfa Aesar and ethyl ether from Honeywell Burdick & Jackson were dried with a column of alumina and dispensed under N_2 from an Innovative Technology Pure Solv system. Benzonitrile and DMSO-d_6 from Aldrich were freeze pump thawed and stored in a glove box. CD_3CN from Cambridge Isotope Labs was freeze pump thawed, dried with molecular sieves and stored in a glove box. $PhP(CH_2OH)_2$ was prepared by reacting $PhPH_2$ from Strem Chemicals with 2 equiv. of *para*-H_2CO from Aldrich. $[Ni(NCMe)_6][BF_4]_2$ [38] and $[Ni(P_2^{Ph}N_2^{Ph})_2][BF_4]_2$ [9] were prepared using literature methods. 4-(Thiophen-3-yl)aniline and thiophene were obtained from Aldrich and used without further purification. Synthesis and manipulation of compounds were performed using standard Schlenk techniques or were done in a glove box.

Solution NMR spectra were recorded on a Varian Inova spectrometer (500 MHz for ^1H). The ^1H chemical shifts were internally calibrated to the CD_2HCN impurity of the deuterated solvent to the value 1.93 ppm. Solid state $^{31}P\{^1H\}$ magic angle spinning (MAS) NMR spectra were collected on a Varian VXR-300 operating at 121.4 MHz using a recycle delay of 200 s and a spin rate of 6150 Hz in a zirconia rotor. All $^{31}P\{^1H\}$ NMR spectra were externally referenced to phosphoric acid. Elemental analysis was done by Columbia Analytical Services using V_2O_5 as a combustion catalyst. The cyclic voltammetry experiments were conducted using a computer aided CHI 1100A potentiostat. The working electrode was a 1 mm glassy carbon PEEK coated electrode from Cypress Systems and was cleaned between scans unless otherwise noted using Gamal from Fisher Scientific on a Buehler microcloth PSA and rinsed with 18 MΩ water. A 3 mm diameter glassy carbon rod from Alfa Aesar was used as an auxiliary electrode. A silver wire pseudo-reference electrode was used with ferrocene as an internal standard. Electrochemistry was done under a nitrogen atmosphere in acetonitrile with NEt_4BF_4 as the electrolyte except for the scan rate current dependence check for **3** which was done in benzonitrile using NBu_4BF_4 as the electrolyte. The nitrogen gas stream was bubbled through acetonitrile to saturate the gas stream for experiments using acetonitrile solutions to minimize solvent loss.

5.2. Preparation of $P_2^{Ph}N_2^{Ar}$

A solution of 4-(thiophen-3-yl)aniline (0.229 g, 1.31 mmol) in acetonitrile (10 mL) was cannula transferred to a Schlenk flask containing a solution of $PhP(CH_2OH)_2$ (0.222 g, 1.30 mmol) in acetonitrile (10 mL) and the mixture was heated to 73 °C for 3 h. A white precipitate started forming after 1 h. The reaction mixture was stirred overnight before removing the solvent under vacuum. Inside a glove box, the white residue was collected on a frit using 20 mL of MeCN to rinse it from the flask and 20 mL of MeCN to wash the solid. The solid was dried under vacuum (0.354 g, 0.572 mmol, 88%). This material was not significantly soluble in any common solvent, but it was sufficiently soluble in DMSO to obtain $^{31}P\{^1H\}$ NMR spectra. $^{31}P\{^1H\}$ MAS NMR (96 MHz, 25 °C) δ −37.3. $^{31}P\{^1H\}$ NMR (DMSO-d_6, 202.3 MHz, 25 °C) δ −49.3 (main resonance), −35.2.

5.3. Preparation of $[Ni(P_2^{Ph}N_2^{Ar})_2NCMe][BF_4]_2$ (**3**)

Solid $P_2^{Ph}N_2^{Ar}$ (0.232 g, 0.375 mmol) and $[Ni(NCMe)_6][BF_4]_2$ (0.091 g, 0.18 mmol) were combined with acetonitrile (15 mL) and stirred for 4 days to give a red solution with a small amount of suspended solid material that was removed by filtration through celite. The solvent was removed under vacuum and the residue was dissolved in 5 mL of acetonitrile. This solution was placed in a container within a larger container with ethyl ether and sealed for slow diffusion giving 0.203 g (0.134 mmol, 74%) of red crystals. A second crop grown the same way from the remaining solution gave 0.018 g (0.011 mmol, 6%) of red crystals. Anal. Calc. for $C_{74}H_{67}B_2F_8N_5NiP_4S_4$: C, 58.83; H, 4.47; N, 4.64. Found: C, 58.49; H, 4.31; N, 5.08%. ^1H NMR (CD_3CN, 500 MHz, 25 °C) δ 7.69 (d, J = 9 Hz, 8H, C-*H* aniline Ph), 7.58 (dd, J = 3.1 Hz, 4H, thiophene), 7.50 (dd, J = 5.3 Hz, 4H, thiophene), 7.46 (dd J = 5.1 Hz, 4H, thiophene), 7.43 (t, J = 8 Hz, 4H, C-*H* P-Ph), 7.36 (m, 8 H, C-*H* P-Ph), 7.27 (d, J = 9 Hz, 8H, C-*H* aniline Ph), 7.21 (t, J = 8 Hz, 8H, C-*H* P-Ph), 4.29 (d, J = 14 Hz, 8H, –C*H*$_2$–), 3.98 (d, J = 14 Hz, 8H, –C*H*$_2$–). $^{31}P\{^1H\}$ NMR (CD_3CN, 202.3 MHz, 25 °C) δ 5.00.

5.4. Proton reduction

5.4.1. Order with respect to acid

A solution of **3** (0.66 mM) and NEt_4BF_4 (0.2 M) in acetonitrile (10.0 mL) was prepared inside a glove box. The volumetric flask was fit with a septum, and 2.0 mL of the solution was syringed into an N_2 purged cell with reference, counter, and working electrodes. The cathodic current for the Ni(II/I) couple was measured to determine i_p. Aliquots of a 0.4 M *p*-cyanoanilinium tetrafluoroborate solution in acetonitrile were added and the current at −0.938 V was measured to determine i_c. The value for i_p was adjusted to compensate for dilution with the addition of the acid solution assuming it is directly proportional to [3] in solution. The ratio of i_c/i_p was plotted against the acid concentration present at each measurement to get a linear relationship indicating the rate of reaction is second order in acid (Fig. 6).

5.4.2. Acid Independent rate

The procedure described in the preceding paragraph was used starting with a 0.73 mM solution of **3** in acetonitrile containing 0.2 M NEt_4BF_4 (1.0 mL) and adding increasingly larger amounts of a 0.41 M solution of *p*-cyanoanilinium tetrafluoroborate in acetonitrile until a total added volume of 2.9 mL was reached. The value of i_c was measured at −0.946 V after each addition. A plot of i_c/i_p vs. [acid] gives a curve that flattens at an i_c/i_p ratio of approximately 24 (see Fig. 7). Using equation 1 and a scan rate of 50 mV/s, a value of 56 s^{-1} was calculated for k.

5.4.3. Order with respect to [3]

A stock solution containing 22 mM *p*-cyanoanilinium tetrafluoroborate and 0.2 M in NEt_4BF_4 in acetonitrile was prepared. A second solution was prepared from this stock solution to produce a solution that was 2.0 mM in **3**. Aliquots of the second solution were added to 1.0 mL of the first stock solution maintaining constant acid and supporting electrolyte concentrations while varying the concentration of **3**. The current i_c was measured at −0.926 V. A plot of i_c vs. [**3**] gives a straight line indicating the rate of reaction is first order in **3**.

5.5. Determination of pK_a of 4-(thiophen-3-yl)aniline

A mixture of 0.014 g (0.08 mmol) 4-(thiophen-3-yl)aniline ($ArNH_2$) and 0.011 g (0.061 mmol) anilinium tetrafluoroborate

was dissolved in 1 mL of CD_3CN and transferred to a NMR tube. The ^1H NMR spectrum of the sample has aromatic peaks at 7.54 and 6.95 ppm assigned to $ArNH_2/ArNH_3^+$ and resonances at 7.32 and 7.04 ppm assigned to $PhNH_2/PhNH_3^+$. A mixture of 0.003 g (0.02 mmol) $ArNH_2$ and 0.048 g (0.15 mmol) 2,6-dichloroanilinium triflate, which has a pK_a of 5.06 [36], was dissolved in 1 mL of CD_3CN, and the ^1H NMR spectrum was acquired to determine chemical shifts of 7.78 and 7.45 ppm for the aromatic resonances of $ArNH_3^+$. Using these chemical shifts and the observed chemical shifts of 7.39 and 6.66 ppm for $ArNH_2$, the mole fraction of unprotonated $ArNH_2$ in the equilibrium mixture was determined to be 0.61 and 0.63 (0.62 average) using each of the aromatic phenyl chemical shifts. The same procedure was used for aromatic *ortho* and *meta* chemical shift values of the $PhNH_2$ located at 7.32 and 7.04 ppm for the equilibrium mixture, 7.53 and 7.39 ppm for $PhNH_3^+$, and 7.08 and 6.63 ppm for $PhNH_2$ to get a mole fraction for $PhNH_2$ of 0.47 and 0.46 (0.46 average). From this data, the equilibrium constant $K_{eq} = [PhNH_2][ArNH_3^+]/[PhNH_3^+][ArNH_2]$ was found to be 0.52. The experiment was repeated twice more using 0.003 g (0.02 mmol) of $ArNH_2$ and 0.003 g (0.02 mmol) $PhNH_3BF_4$ as well as 0.010 g (0.057 mmol) of $ArNH_2$ and 0.007 g (0.04 mmol) of $PhNH_3BF_4$ to get K_{eq} values of 0.52 and 0.53, respectively. The pK_a of $ArNH_3^+$ is the sum of the pK_a of $PhNH_3^+$ and log K_{eq}. Using the pK_a value of $PhNH_3^+$ to be 10.62 [37] and the average K_{eq} of 0.52, the pK_a of $ArNH_3^+$ is 10.34.

5.6. Electrochemical oxidation of **3**

The potential of a glassy carbon electrode in a benzonitrile solution containing 0.93 mM **3**, 0.2 M NBu_4BF_4, and ≈1 mM ferrocene was scanned from −0.5 V to 0.2 V at 0.1 V/s and a reversible Fc^+/Fc wave was observed. Without cleaning the electrode, a second cyclic voltammogram was recorded in which the potential was scanned from −0.5 V to 1.7 V and back to −0.5 V at 0.1 V/s. The anodic wave for ferrocene oxidation was the same for both scans and was used to reference the voltammogram.

For investigation of potential required to coat the working electrode as a result of oxidation of **3**, cyclic voltammograms were recorded on an acetonitrile solution containing 1.0 mM **3** and 0.1 M NEt_4BF_4 in which the potentials were initially swept in the negative direction to observe the Ni(II/I) and Ni(I/0) couples and then reversed and scanned to increasingly more positive potentials using a scan rate of 0.1 V/s. A second scan was then recorded to observe any change in current from the initial cycle. Sequential cyclic voltammograms scanned to a maximum of 0.6 V in the positive direction had similar peak currents for ferrocene and Ni(II/I) and Ni(I/0) waves with no change in potentials. However, a similar cyclic voltammogram scanned initially to 0.7 V resulted in decreased and broadened waves for the Ni(II/I) and Ni(I/0) couples for subsequent scans compared to those seen before the cycling to 0.7 V. Cycling to 0.8 V resulted in significant changes for the Ni reduction peaks observed in subsequent cyclic voltammograms. Cycling to 1.1 V at 0.1 V/s resulted in no observed current for the Ni(II/I) and Ni(I/0) couples in subsequent cyclic voltammograms.

5.7. Scan rate dependence

An acetonitrile solution containing 0.5 mM **3** and 0.1 M NEt_4BF_4 was used in series of cyclic voltammograms with an initial potential of −0.4 V, sweeping to −1.4 V, then to 1.6 V, and finally back to −0.4 V at 0.1 V/s. A subsequent cyclic voltammogram from −0.4 V to −1.4 V and back to −0.4 V had no observable current for previously observed Ni(II/I) and Ni(I/0) couples. After cleaning the working electrode the experiment was repeated at 0.2 and 0.5 V/s with the same result. After cleaning the working electrode the experiment was repeated at 1 V/s for the initial scan and 0.1 V/s for the follow up cyclic voltammogram between −0.4 and −1.4 V. In this case, waves corresponding to the Ni(II/I) and Ni(I/0) couples of **3** were observed, but they were broadened and the current was diminished from the initial scan.

5.8. Electrode transfer experiments

In this experiment two electrochemical cells were used. One cell contained a solution of **3** as described in the preceding paragraph. A second cell contained a 0.1 M solution of NEt_4BF_4 in acetonitrile, but no **3**. After various coating experiments described in the preceding paragraph using solutions containing **3**, the working electrode was placed in the second cell containing a solution with the electrolyte, but no dissolved **3**, and scanned to −1.4 V. No observable current was observed for Ni(II/I) or Ni(I/0) couples above the baseline current of the cyclic voltammogram.

5.9. Copolymerization with thiophene

A cyclic voltammogram was recorded on an acetonitrile solution (3.0 mL) containing 0.6 mM **3** and 0.1 M in NEt_4BF_4. The initial potential was −0.41 V, and the potential was swept to −1.41 V, then to 1.59 V, and back to −0.41 V at 0.1 V/s. Thiophene (5 μL, 0.062 mmol, 20 mM) was added to the cell and mixed by bubbling with N_2 gas. Another cyclic voltammogram was recorded at 0.1 V/s over the same potential range. Upon sweeping in the positive direction, the onset of oxidative current was observed at 0.6 V similar to the cyclic voltammograms recorded in the absence of thiophene. However, at 1.2 V the very large oxidation currents were observed. On the return negative scan to −0.41 V, a peak at 0.54 V was observed. Scanning the same range again without cleaning the working electrode showed no reduction current for Ni(II/I) and Ni(I/0) couples, but increasing anodic current between 0.1 and 1.59 V and cathodic current between 1.23 and −0.41 V. This process was repeated 9 more times sequentially with similar effect (Fig. 4).

A similar experiment was performed using 3 mL acetonitrile solutions containing 0.9 mM **3**, 0.1 M NEt_4BF_4, and 40 mM thiophene. The coating of the electrode was done with a single scan in the range outlined above at 0.1, 0.2, 0.5, and 1 V/s. The coated working electrode was then placed in a CV cell containing a 0.1 M NEt_4BF_4 MeCN solution and a scan performed over the same range as above. Polythiophene was observed at potentials positive of 0.2 V but no Ni reduction peaks were observed.

5.10. Attempted mediation with $CoCp_2PF_6$

A cell containing a solution of 0.7 mM **3** and 0.2 M NEt_4BF_4 in MeCN was used for coating the working electrode with a single scan to 1.8 V at 0.1 V/s before placing the working electrode in a second cell containing 0.2 M NEt_4BF_4 and 7 mM $CoCpPF_6$ in acetonitrile. A cyclic voltammogram was recorded from −0.2 V to −1.2 V and back to −0.2 V. Only the reversible couple for Co(III)/Co(II) was observed with no enhanced cathodic current compared to the anodic current.

5.11. Cyclic voltammogram of **2c**

An acetonitrile solution containing 0.68 mM **2c**, 0.2 M NEt_4BF_4, and ferrocene was scanned from −0.22 V to −1.22 V, back to 1.78 V, and finally to −0.22 V at 0.1 V/s. The Ni(II/I) and Ni(I/0) waves matched those previously reported. The ferrocenium/ferrocene couple was reversible and irreversible oxidations of **2c** were observed beginning at 0.6 V.

Acknowledgements

This research was supported by the Laboratory Directed Research and Development Program of the Pacific Northwest National Laboratory. The Pacific Northwest National Laboratory is operated by Batelle for the US Department of Energy.

References

[1] W. Lubitz, W. Tumas (Eds.), Chem. Rev. 107 (10) (2007).
[2] M. Frey, ChemBioChem 3 (2002) 153–160.
[3] J.W. Peters, Curr. Opin. Struct. Biol. 9 (1999) 670–676.
[4] J.W. Peters, W.N. Lanzilotta, B.J. Lemon, L.C. Seefeldt, Science 282 (1998) 1853–1858.
[5] Y. Nicolet, A.L. de Lacey, X. Vernède, V.M. Fernandez, E.C. Hatchikian, J.C. Fontecilla-Camps, J. Am. Chem. Soc. 123 (2001) 1596–1601.
[6] J.C. Fontecilla-Camps, A. Volbeda, C. Cavazza, Y. Nicolet, Chem. Rev. 107 (2007) 4273–4303.
[7] S. Shima, O. Pilak, S. Vogt, M. Schick, M.S. Stagni, W. Meyer-Klaucke, W. Warkentin, R.K. Thauer, U. Ermler, Science 321 (2008) 572–575.
[8] C.J. Curtis, A. Miedaner, R.F. Ciancanelli, W.W. Ellis, B.C. Noll, M.R. DuBois, D.L. DuBois, Inorg. Chem. 42 (2003) 216–227.
[9] A.D. Wilson, R.H. Newell, M.J. McNevin, J.T. Muckerman, M.R. DuBois, D.L. DuBois, J. Am. Chem. Soc. 128 (2006) 358–366.
[10] A.D. Wilson, R.K. Shoemaker, A. Miedaner, J.T. Muckerman, D.L. DuBois, M. Rakowski DuBois, Proc. Natl. Acad. Sci. 104 (2007) 6951–6956.
[11] K. Fraze, A.D. Wilson, A.M. Appel, M. Rakowski DuBois, D.L. DuBois, Organometallics 26 (2007) 3918–3924.
[12] M. Rakowski DuBois, D.L. DuBois, C.R. Chim. 11 (2008) 805–817.
[13] M. Rakowski DuBois, D.L. DuBois, Chem. Soc. Rev. 38 (2009) 62–72.
[14] J.W. Raebiger, A. Miedaner, C.J. Curtis, S.M. Miller, O.P. Anderson, D.L. DuBois, J. Am. Chem. Soc. 126 (2004) 5502–5514.
[15] C.J. Curtis, A. Miedaner, J.W. Raebiger, D.L. DuBois, Organometallics 23 (2004) 511–516.
[16] D.E. Berning, A. Miedaner, C.J. Curtis, B.C. Noll, M.C. Rakowski DuBois, D.L. DuBois, Organometallics 20 (2001) 1832–1839.
[17] M.R. Nimlos, C.H. Chang, C.J. Curtis, A. Miedaner, H.M. Pilath, D.L. DuBois, Organometallics 27 (2008) 2715–2722.
[18] G.M. Jacobsen, R.K. Shoemaker, M. Rakowski DuBois, D.L. DuBois, Organometallics 26 (2007) 4964–4971.
[19] A.D. Wilson, K. Fraze, B. Twamley, S.M. Miller, D.L. DuBois, M. Rakowski DuBois, J. Am. Chem. Soc. 130 (2008) 1061–1068.
[20] R.W. Murray (Ed.), Molecular Design of Electrode Surfaces; Techniques of Chemistry, vol. XXII, John Wiley & Sons, New York, 1992.
[21] C.P. Mehnert, E.J. Mozeleski, R.A. Cook, Chem. Commun. (2002) 3010–3011.
[22] D.L. DuBois, Inorg. Chem. 23 (1984) 2047–2052.
[23] G. Guerrero, P.H. Mutin, A. Vioux, Chem. Mater. 13 (2001) 4367–4373.
[24] R. Back, R.B. Lennox, Langmuir 8 (1992) 959–964.
[25] B. Ulgut, H.D. Abruña, Chem. Rev. 108 (2008) 2721–2736.
[26] V.G. Märkl, G.Y. Jin, C. Schoerner, Tetrahedron Lett. 21 (1980) 1409–1412.
[27] S.A. Trammell, T.J. Meyer, J. Phys. Chem. B 103 (1999) 104–107.
[28] F. Cecchet, M. Marcaccio, M. Margotti, F. Paolucci, S. Rapino, P. Rudolf, J. Phys. Chem. B 110 (2006) 2241–2248.
[29] F. Trudeau, F. Daigle, D. Leech, Anal. Chem. 69 (1997) 882–886.
[30] A.M. Appel, S.-J. Lee, J.A. Franz, D.L. DuBois, M. Rakowski DuBois, B. Twamley, Organometallics 28 (2009) 749–754.
[31] G.A.N. Felton, R.S. Glass, D.L. Lichtenberger, D.H. Evans, Inorg. Chem. 45 (2006) 9181–9184.
[32] J.Y. Yang, R.M. Bullock, W.J. Shaw, B. Twamley, K. Fraze, M. Rakowski DuBois, D.L. DuBois, J. Am. Chem. Soc. 131 (2009), doi: 10.1021/ja900483x.
[33] R.S. Nicholson, I. Shain, Anal. Chem. 36 (1964) 706.
[34] J.M. Savéant, E. Vianello, Electrochim. Acta 10 (1965) 905–920.
[35] J.M. Savéant, E. Vianello, Electrochim. Acta 12 (1967) 629–646.
[36] D. Berning, B. Noll, D. DuBois, J. Am. Chem. Soc. 121 (1999) 11432–11447.
[37] I. Kaljurand, A. Kütt, L. Sooväli, T. Rodima, V. Mäemets, I. Leito, I.A. Koppel, J. Org. Chem. 70 (2005) 1019–1028.
[38] B.J. Hathaway, A.E. Underhill, J. Chem. Soc. (1960) 3705–3711.